Intelligent Radio Resource Management in Reconfigurable IRS-enabled NOMA Networks

***Abstract*—Intelligent reflecting surfaces (IRSs) are anticipated to provide reconfigurable propagation environment for next generation communication systems. In this paper, we investigate a downlink IRS-aided multi-carrier (MC) non-orthogonal multiple access (NOMA) system, where the IRS is deployed to especially assist the blocked users to establish communication with the base station (BS). To maximize the system sum rate under network quality-of-service (QoS) and rate fairness constraints, we formulate a problem for joint optimization of sub-channel assignment and power allocation. The formulated problem is mixed non-convex. Therefore, a novel two stage algorithm is proposed for sub-channel assignment and power allocation. Firstly, the sub-channel assignment problem is solved by one-to-one stable matching algorithm. Then, the power allocation problem is solved under the given sub-channel using Lagrangian dual decomposition method based on Lagrangian multipliers. The simulated results demonstrate that the proposed approach outperforms the benchmark approaches in terms of network sum rate and user fairness and the performance of the proposed approach can be enhanced by increasing the number of IRS reflecting elements. It is further shown that for proposed algorithm, a smaller fairness factor provides a greater user fairness.**

***Index terms*—Intelligent reflecting surface, non-orthogonal multiple access, resource allocation, optimization, stable matching.**

I. Introduction

THE demand for beyond fifth generation (B5G) communication systems having high energy and spectrum efficiency is rapidly growing [1]. Various sophisticated wireless technologies including millimeter wave (mmWave) and massive multiple-input multiple output (MIMO), have been proposed in this regard [2]. However, these technologies provide performance improvement at the expense of high hardware cost and power consumption. Moreover, these technologies lack control over the propagation channel, which is highly stochastic, hence they do not guarantee quality-of-service (QoS) under poor propagation conditions, i.e, blockage of wireless links and severe attenuation.

Recently, a cost and energy efficient technology called intelligent reflecting surfaces (IRSs) has been proposed for B5G communications [3], [4]. Specifically, IRS is a reconfigurable planer surface consisting of a large number of passive reflecting elements. By intelligently tuning these elements, a favorable propagation environment can be established between the transmitter and the receiver [5]. Compared to conventional active relaying or beamforming, IRS passively reflects the signal without requiring signal generation or amplification [5]. Thus, IRS provides superior performance at reduced hardware cost and power consumption [6], [7].

On the other hand, non-orthogonal multiple access (NOMA) has been recognized as a effective technology where power-domain NOMA (PD-NOMA) enables multiple users to share the same resource (e.g., time, frequency, code) block, and hence provides both spectral and energy efficiency [8], [9]. In a downlink NOMA system, superposition coding (SC) is used at the base station (BS) to multiplex the data of the users with different channel gains and successive interference cancellation (SIC) is deployed at the receiver to decode the message signals [10].

The conventional NOMA system lacks the control over the channel conditions of the users. Inspired by this, in this paper, we investigate the performance of IRS-aided multi-carrier (MC) NOMA system by employing the IRS to enable multiple paths to the users to provide strong composite channel gains. In the sequel, we introduce some relevant research in these areas.

A. Literature Review

*1) **Literature on NOMA**:* In [11], [12], it has been demonstrated that NOMA shows superior performance than the orthogonal multiple access (OMA) in terms of outage probability and ergodic capacity. Similarly, in [13], the authors signified the superiority of NOMA over OMA under different channel gains for a fair power allocation scheme. NOMA has been studied extensively both in single-carrier (SC) and multi-carrier (MC) communication systems. To maximize the system throughput and energy efficiency, the authors of [14] and [15], respectively, jointly optimize the sub-carrier and power allocation.

*2) **Literature on IRS**:* IRS has gained considerable attention both in academia and industry over the recent few years. Not only in wireless communication systems, IRS has proven to be a beneficial technology in optical communication systems. The authors in [16] have revealed that outage probability of optical communication system can be reduced through IRS assistance. The path loss model for IRS aided communication system has been derived using physical optics techniques in [17]. In [18], the authors have demonstrated that IRS can achieve high data rate with increased number of IRS elements at low power consumption as compared to decode and forward (DF) technology. The channel estimation of IRS-assisted communication systems has been studied in [19], [20] where the authors have proposed least square (LS) based estimation and minimum mean square error (MMSE) estimation in [19] and [20], respectively. The IRS is compatible with other advanced technologies such as mmWave communication, unmanned aerial vehicle (UAV) networks [21], backscatter communication [22], simultaneous wireless information and power transfer (SWIPT) [23] and physical layer secrecy [24].

*3) **Literature on IRS-assisted NOMA**:* Both IRS and NOMA are promising technologies for B5G communication systems. Combination of both technologies can enhance system coverage and energy efficiency. The co-existence of IRS and NOMA has been studied recently [25]–[31]. In [25], the impact of coherent and random phase shifting designs for IRS-assisted NOMA system has been studied. The authors have developed analytical results for the comparison of two phase shifting designs. The authors in [26] formulated a power minimization problem for IRS-aided single-input single-output (SISO) NOMA system and optimize the phase shifts introduced by IRS. Similar problem has been investigated by the authors of [27] for IRS-aided multiple-input single-output (MISO) NOMA system. To address the hardware limitations, the authors in [28] presented a simple design for IRS-aided NOMA network. In [29], sum-rate maximization problem for ideal and non-ideal IRSs has been analyzed through joint optimization of active and passive beamforming vectors. In [30], the closed-form expressions for outage probability and ergodic capacity are derived for IRS-aided SISO NOMA network. As a further enhancement, the authors in [31] derive the outage probability and ergodic capacity expressions for IRS-NOMA network with both perfect and imperfect SIC and compared the performance of IRS-NOMA with IRS-OMA and other relaying technologies. The authors have demonstrated that IRS-NOMA outperforms the benchmarking schemes with the increased number of IRS elements.

B. Contributions

To the best of our knowledge, there is no prior work on joint channel and power allocation for IRS-aided downlink MC-NOMA network that ensures fairness and per user QoS requirement. In this paper, we consider an IRS-aided downlink MC-NOMA network where a BS assigns a single sub-channel to each NOMA cluster. Thus, all users within the cluster share the sub-channel. Moreover, we investigate the NOMA fairness issue due to which weak users in the cluster are deprived of good services. Our proposed approach makes sure that all users in the cluster experience similar services hence ensuring fairness. The contributions of this paper are summarized as follows

- To optimize the sub-channel assignment and power allocation, we formulate a problem to maximize the sum rate of the network, subject to transmit power constraint of the BS, the available channels at the BS, the per user QoS requirement and network fairness constraint to balance the rates of the users. However, the formulated problem is challenging to solve jointly because of the nature of optimization variables.
- We decouple the sum rate maximization problem into two parts: sub-channel assignment and power allocation. Firstly, sub-channel assignment problem is solved using matching theory followed by power allocation using Lagrangian method. The sub-channel allocation problem is formulated as one-to-one two sided stable matching problem, where the sub-channel assignment is based on the preferences of the clusters such that each cluster is assigned a single unique sub-channel. The power allocation problem is solved by first applying the Karush-Kahn-Tuck (KKT) conditions to Lagrangian function to determine the Lagrangian multipliers and then using the sub-gradient method to achieve convergence.
- Finally, we demonstrate that the proposed approach ensures user fairness and achieves greater network sum rate. The performance of the proposed approach can be enhanced by increasing the number of IRS reflecting elements.

The rest of the paper is organized as follows. The system model description is presented in Section II. In Section III, we formulate the joint sub-channel assignment and power allocation problem for sum rate maximization. Section IV discusses the proposed sub-channel assignment algorithm while Section V presents the proposed power allocation algorithm. The simulated results and their discussion are presented in Section VI. Finally, Section VII presents the conclusion.

II. System Model

As illustrated in Fig. 1, we consider an IRS-aided downlink MC-NOMA communication system, where a macro BS equipped with a single transmit antenna and an IRS equipped with *N* reconfigurable passive reflecting elements serve *K* uniformly distributed single-antenna users. The IRS is connected to a smart controller, which communicates with the BS and changes the phase of the incident signal. The *K* users are grouped into *M* clusters, denoted by $\mathcal{M} = \{1, 2, \ldots, M\}$, where $K \geq M$. We assume that the direct links from the BS to users are strongly attenuated for some clusters, due to the blocking objects, hence such users take help from the IRS to establish communication. On the other hand, some clusters have strong and direct BS to user links such that the signal received via IRS is negligible because of the increased path loss. Let $\mathcal{K}_m = \{1, 2, \ldots, K_m\}$ denotes the set of users in cluster *m* and $K_m = \mid \mathcal{K}_m \mid$ denotes the maximum number of users in cluster *m*, where K_m ranges from $2 \leq K_m \leq K$ and $\mid \mathcal{K}_m \mid$ denotes the cardinality of set $\mathcal{K}_m$. For notation simplicity, we define $\mathcal{U}_k^m$ as the *k-th* user of cluster *m*, where $m \in \mathcal{M}$ and $k \in \mathcal{K}_m$. The total system bandwidth, *B*, is equally divided into C sub-channels, each of bandwidth $W = B/M$, implying that each NOMA cluster is allocated a single sub-channel. Hence all users in a cluster share the same sub-channel. The sub-channel occupancy of user $\mathcal{U}_k^m$ in sub-channel c is denoted by $\lambda_k^m[c]$, where $\lambda_k^m[c] \in \{0, 1\}$ and $\lambda_k^m[c] = 1$ indicates that sub-channel c is occupied by user $\mathcal{U}_k^m$, otherwise $\lambda_k^m[c] = 0$.

The power allocated to user $\mathcal{U}_k^m$ over the sub-channel c is denoted by $p_k^m[c]$, satisfying $\sum_{k=1}^{K_m} p_k^m[c] \leq P_c$ and $P_c = P_{BS}/C$, where P_c is the power allocated to sub-channel *c* and P_{BS} is the total transmit power of the BS. According to the NOMA principle, the BS transmits the superimposed signal $S^m[c]$ to K_m users of cluster *m* over the sub-channel *c*, such that

$$S^m[c] = \sum_{k=1}^{K_m} \lambda_k^m[c] \sqrt{p_k^m[c]} s_k^m[c], \tag{1}$$

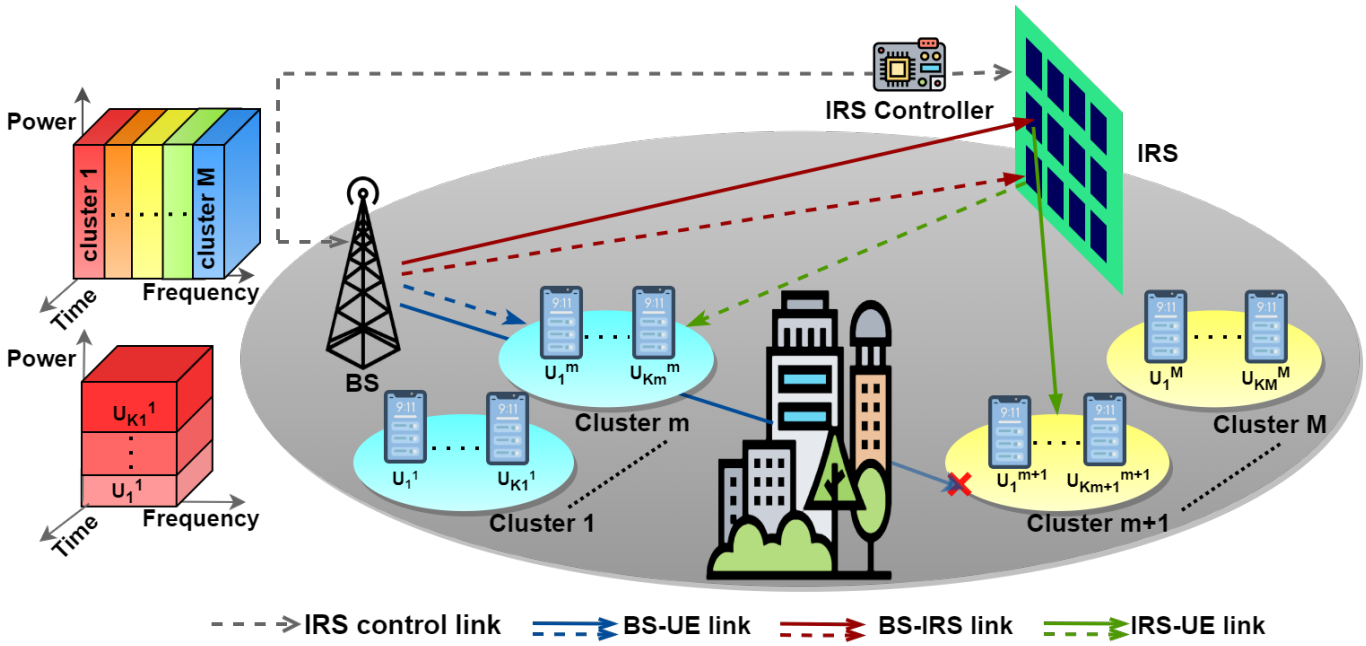

Fig. 1. System model of IRS-aided downlink MC-NOMA network.

where $s_k^m[c]$ is the message signal for $\mathcal{U}_k^m$ over the sub-channel c. The signal $s_k^m[c]$ is assumed to be zero mean with unit variance, i.e., $\mathbb{E}\{|\ s_k^m[c]\ |^2\} = 1$, where $\mathbb{E}\{.\}$ is the expectation operator. The received signal at $\mathcal{U}_k^m$ over sub-channel c is given as

$$y_k^m[c] = \left[\frac{r_k^m[c]}{\sqrt{L\left(d_k^m\right)}} + \frac{\mathbf{g}_k^m[c]^H\,\Theta\,\mathbf{G}[c]}{\sqrt{L\left(d_r\right)L\left(\widehat{d}_k^m\right)}}\right] S^m[c] + n_k^m[c], \tag{2}$$

where Θ = diag $\left(\beta_1 e^{j\theta_1}, \beta_2 e^{j\theta_2}, \ldots, \beta_N e^{j\theta_N}\right) \in \mathbb{C}^{N\times N}$, is a diagonal matrix, $\beta_n \in [0,1]$ and $\theta_n \in [0, 2\pi]$ denote the amplitude reflection coefficient and the phase shift of the *n-th* reflecting element of the IRS, respectively [5], [28]. Similarly in (2), $\mathbf{g}_k^m[c] \in \mathbb{C}^{N\times 1}$ denotes the channel response matrix from the IRS to $\mathcal{U}_k^m$ over the sub-channel c, $\mathbf{G}[c] \in \mathbb{C}^{N\times 1}$ denotes the channel response matrix from the BS to the IRS over the sub-channel c, $r_k^m[c]$ and d_k^m denote the channel coefficient over the sub-channel c and the distance from the BS to $\mathcal{U}_k^m$, respectively and d_r denotes the distance from the BS to the IRS. Similarly, $\widehat{d}_k^m$ denotes the distance from the IRS to $\mathcal{U}_k^m$, $n_k^m[c] \sim \mathcal{CN}\left(0, \sigma^2\right)$ is the additive white Gaussian noise (AWGN) at $\mathcal{U}_k^m$ over the sub-channel c and $L(d)$ is the effective path loss expressed as

$$L(d)\,[dB] = 35.1 + 36.7\log_{10}(d) - G_t - G_r, \tag{3}$$

where $d \in \{d_k^m, d_r, \widehat{d}_k^m\}$, G_t and G_r are the antenna gains at the transmitter and receiver, respectively.

We assume that all channels are complex Gaussian distributed with zero mean and unit variance, i.e., $\mathcal{CN}(0,1)$. A perfect channel state information (CSI) for all channels is available at the BS, which leads us to use coherent phase shifting design for IRS [25]. Hence θ_n is selected as

$$\theta_n = arg\left(r_k^m[c]\right) - arg\left(\left[\mathbf{g}_k^m[c]\right]_n\left[\mathbf{G}[c]\right]_n\right), \tag{4}$$

where $\left[\mathbf{g}_k^m[c]\right]_n$ and $\left[\mathbf{G}[c]\right]_n$ represent the *n-th* element of $\mathbf{g}_k^m[c]$ and $\mathbf{G}[c]$, respectively.

Without the loss of generality, the users in each cluster are ordered based on their composite downlink channel. Specifically, the K_m users in cluster m are ordered as

$$|\ h_1^m[c]\ |^2 \geq |\ h_2^m[c]\ |^2 \geq \ldots \geq |\ h_{K_m}^m[c]\ |^2, \tag{5}$$

where $h_k^m[c] = \frac{r_k^m[c]}{\sqrt{L\left(d_k^m\right)}} + \frac{\mathbf{g}_k^m[c]^H\,\Theta\,\mathbf{G}[c]}{\sqrt{L(d_r)L\left(\widehat{d}_k^m\right)}}$.

The power allocation principle of NOMA implies $p_1^m[c] \leq p_2^m[c] \leq \ldots \leq p_{K_m}^m[c]$, i.e., the highest channel gain user (the strongest user) gets the lowest power and vice versa. Hence, the user with the lowest channel gain (the weakest user), i.e., of $\mathcal{U}_{K_m}^m$, directly decodes its signal by treating the other users' signals as interference. While the the strongest user, i.e., $\mathcal{U}_1^m$, performs SIC to cancel interference from other users and decodes its signal without interference. Thus, the user $\mathcal{U}_k^m$ decodes its signal by successfully cancelling the interference from users $\{\mathcal{U}_{k+1}^m, \mathcal{U}_{k+2}^m, \ldots, \mathcal{U}_{K_m}^m\}$. The achievable data rate at $\mathcal{U}_k^m$ over the sub-channel c is given by

$$R_k^m[c] = \log_2(1 + SINR_k^m[c]), \tag{6}$$

where the SINR at $\mathcal{U}_{m,k}$ is

$$SINR_k^m[c] = \frac{\lambda_k^m[c]\ |\ h_k^m[c]\ |^2\ p_k^m[c]}{|\ h_k^m[c]\ |^2\ I_k^m[c] + \sigma^2}, \tag{7}$$

where $I_k^m[c] = \sum_{i=1}^{k-1} \lambda_k^m[c] p_i^m[c]$ denotes the total interference power at $\mathcal{U}_k^m$ from users $\{\mathcal{U}_1^m, \mathcal{U}_2^m, \ldots, \mathcal{U}_{k-1}^m\}$.

In downlink NOMA system, for successful SIC process, all users must satisfy the minimum power gap as [32]

$$p_k^m[c] \mid h_{k-1}^m[c] \mid^2 - \sum_{i=1}^{k-1} p_i^m[c] \mid h_{k-1}^m[c] \mid^2 \geq \beta, \tag{8}$$

where β denotes the minimum power gap between the users in each cluster.

The achievable cluster sum rate over sub-channel c is given by

$$R_{sum}^m[c] = \sum_{k=1}^{K_m} R_k^m[c], \tag{9}$$

III. Problem Formulation

We formulate the sum rate maximization problem under QoS and rate balancing fairness constraints for sub-channel and power allocation as follows

$$\begin{aligned}
&(\mathbf{P}): \underset{\lambda_k^m[c],\, p_k^m[c]}{\text{maximize}} \sum_{k=1}^{K_m}\sum_{c=1}^{C} \lambda_k^m[c] R_k^m[c] \\
&\text{subject to:} \\
&C_1: \lambda_k^m[c] R_k^m[c] \geq R_{min}\,, \forall\, k, m, c \\
&C_2: \sum_{c=1}^{C}\sum_{k=1}^{K_m} \lambda_k^m[c] p_k^m[c] \leq P_c = P_{BS}/C, \forall\, m \\
&C_3: \lambda_k^m[c] p_k^m[c] \geq 0\,, \forall\, k, m, c \\
&C_4: \sum_{c=1}^{C} \lambda_k^m[c] \left(\sum_{i=1}^{k-1} p_i^m[c] + \frac{\beta}{\mid h_{k-1}^m[c] \mid^2} \leq p_k^m[c] \right), \forall\, k, m \\
&C_5: \lambda_k^m[c] \in \{0,1\}, \forall\, k, m, c \\
&C_6: \sum_{c=1}^{C} \lambda_k^m[c] = 1, \forall\, k, m \\
&C_7: \sum_{k=1}^{K_m} \lambda_k^m[c] = K_m, \forall\, m, c \\
&C_8: \lambda_k^m[c]\big(R_1^m[c] - R_k^m[c] \big) \leq \delta, \forall\, k, m, c
\end{aligned} \tag{10}$$

In the optimization problem **(P)**, the objective function is to maximize the sum rate of the cluster m. The constraint C_1 denotes the QoS requirement for each user, i.e., the achievable rate must be greater than the minimum rate requirement. We assume that the minimum rate requirement is same for all users in the network. The constraint C_2 limits the total available power of the BS. The constraint C_3 ensures the non-negative transmit power of all users. The constraint C_4 guarantees the successful completion of SIC process, where β denotes the minimum power difference among the different users to apply SIC. The constraint C_5 is an indicator function of sub-channel c occupied by the user $\mathcal{U}_k^m$, where $\lambda_k^m[c] = 1$ indicates that sub-channel c is occupied by user $\mathcal{U}_k^m$, otherwise $\lambda_k^m[c] = 0$. The constraint C_6 represents that each user can access only one sub-channel and the constraint C_7 represents that one sub-channel serves K_m users, implying that all users in the cluster share the same sub-channel. Finally, C_8 is the fairness constraint, that ensures minimum difference between the achievable rates of the strongest user, i.e., $\mathcal{U}_1^m$, and the other users within the cluster, where δ denotes the maximum rate difference. The parameter δ indicates, how fair the system capacity is shared among the users and it can be adjusted according to the requirement. The purpose of this constraint is to balance the rates of all users in the cluster, hence ensuring fairness, i.e., when δ gets close to 0, the achievable rate of each user gets close to each other. We assume that the parameter δ is same for all clusters.

The sum rate maximization problem in **(P)** is a mixed non-convex problem with the discrete variables $\lambda_k^m[c]$ and continuous variables $p_k^m[c]$. Therefore, **(P)** cannot be directly solved using traditional convex optimization methods [33]. Hence, we solve the problem in two stages for sub-channel and power allocation. Firstly, the sub-channel allocation problem is solved using the *matching theory*. Then the power allocation problem is solved for the given channel allocation using Lagrangian method.

IV. Proposed Solution for Sub-Channel Assignment

In this section, we present a sub-channel assignment scheme based on matching theory. The sub-channel assignment problem is to find the best match between the clusters and the sub-channels. The BS first assumes that the total available power is equally allocated to all sub-channels. The maximum power allocated to each cluster is P_c. The minimum power requirement, $\widehat{p}_k^m[c]$, of each user on each channel, to satisfy R_{min}, can be determined using (6). Hence the total minimum power requirement of each cluster on each channel is $P_{min}^m[c] = \sum_{k=1}^{K_m}\sum_{c=1}^{C} \lambda_k^m[c]\widehat{p}_k^m[c]$. The initial power allocation is performed using the available set of power factors, taking into account the NOMA principle, and the minimum and maximum power constraints. Then sub-channel assignment is performed using matching theory. The original problem **(P)** can be simplified for sub-channel assignment as follows

$$\begin{aligned}
&(\mathbf{P1}): \underset{\lambda_k^m[c]}{\text{maximize}} \sum_{k=1}^{K_m}\sum_{c=1}^{C} \lambda_k^m[c] R_k^m[c] \\
&\text{subject to:} \\
&\overline{C}_1: \lambda_k^m[c] \in \{0,1\}, \forall\, k, m, c \\
&\overline{C}_2 \sum_{c=1}^{C} \lambda_k^m[c] = 1, \forall\, k, m \\
&\overline{C}_3: \sum_{k=1}^{K_m} \lambda_k^m[c] = K_m, \forall\, m, c
\end{aligned} \tag{11}$$

It is noted that the problem **(P1)** is one-to-one two sided matching problem, as each cluster is assigned a single unique sub-channel and each sub-channel is allocated to a single cluster. The proposed stable matching algorithm is presented in the next section.

A. One-to-One Two-sided Matching Problem Formulation

To develop an efficient sub-channel allocation algorithm, we consider the clusters and channels as two sets and the objective is to match the clusters to sub-channel such that

Algorithm 1 The Proposed Stable Matching Algorithm for Sub-Channel Allocation

Input: $\mathcal{M}, \mathcal{C}$ and $\mathcal{Q}$

Step 1: Initialization

(a) Establish a list of proposals $\{T\}$ that each sub-channel receives from the clusters.

(b) Each cluster sets its preference list $R(m)$ through $\mathcal{Q}$.

Step 2: Matching Algorithm

(a) Each cluster $m \in \mathcal{M}$ proposes to its most preferred sub-channel in $R(m) : c = \arg \min_{c \in R(m)} Q^m[c], \forall m \in M$.

(b) If $\mid T(c) \mid = 1$, then c is matched to *m*.

(c) If $\mid T(c) \mid > 1$, then c chooses one cluster randomly from the list of proposals $\{T(c)\}$ and rejects rest of the clusters.

(d) The rejected clusters remove c from their preference lists.

(e) If all clusters are matched to sub-channels, go to Step 3, else go back to Step 2(a) for clusters that have been rejected by some sub-channel.

Step 3: End of the algorithm.

Output: $\forall\, m \in \mathcal{M}$, $\forall\, c \in \mathcal{C}$, output $\Phi(m) = c$

constraints in (11) are satisfied. A matching is defined as an allocation of sub-channels in $\mathcal{C}$ to clusters in $\mathcal{M}$, where each cluster is assigned a distinct sub-channel. Explicitly it is defined as follows

Definition 1: Consider two disjoint sets, $\mathcal{M} = \{1, 2, \ldots, M\}$ of the clusters, and $\mathcal{C} = \{1, 2, \ldots, C\}$ of the sub-channels, a one to one matching Φ is defined as an injection from $\mathbb{I} = \mathcal{M} \cup \mathcal{C}$ to $\mathbb{I}$ with following properties:

1. $\Phi \circ \Phi(y) = y,\ \forall\, y \in \mathbb{I}$

2. $\Phi(m) \in \mathcal{C},\ \forall\, m \in \mathcal{M}$

3. $\Phi(c) \in \mathcal{M},\ \forall\, c \in \mathcal{C}$

4. $\forall\, c \in \mathcal{C}\ \ \exists\, y \in \mathcal{M}$ s.t. $\Phi(y) = c$

The first property states that the matching is one-to-one in a way that each cluster is allocated a distinct sub-channel. Here, it should be noted that the users within the cluster share the sub-channel. The second property ensures that for each cluster, its matched element exists in the set of sub-channels. Similarly, the third property ensures that for each sub-channel, its matched element exists in the set of clusters. Lastly, each sub-channel should have a cluster matched to it, such that no resources are wasted.

The specific matching outcome is the result of matching mechanism, which maps the preferences of clusters and sub-channels. The preference relation is described as follows [34].

Definition 2: Consider a set $\mathcal{W}$ and a binary relation $\succeq$. The binary relation $\succeq$ is complete if for all $w, v \in \mathcal{W}$, either $w \succeq v$ or $v \succeq w$ (or both). A binary relation is transitive if $w \succeq v$ and $v \succeq u$ implies that $w \succeq u$. A binary relation that is complete and transitive is a (weak) preference relation.

The preference of clusters over the set of sub-channels is based upon the difference between the rates of strongest and weakest users in the cluster. The difference between the rates of $\mathcal{U}^m_{K_m}$ and $\mathcal{U}^m_1$ over the sub-channel c is expressed as

$$Q^m[c] = \mid R^m_{K_m}[c] - R^m_1[c] \mid, \tag{12}$$

The set of all $Q^m[c]$ is denoted as $\mathcal{Q}$. The cluster *m* prefers the sub-channel for which $Q^m[c]$ is minimum. Note that each cluster utilizes one sub-channel. The set of preference lists of clusters is denoted as

$$\mathcal{R} = \{R(1), \ldots, R(M)\} \tag{13}$$

The relations of preference over the sub-channels can be represented as

$$c \succeq_m c' \Leftrightarrow\ Q^m[c] < Q^m[c'], \tag{14}$$

which implies that the cluster *m* prefers the sub-channel c over the the sub-channel c' because the sub-channel c provides smaller difference between the rates of strongest and weakest users. The clusters utilize their preferences over the sub-channels in order to send proposals. Here we assume that the sub-channels do not have any preference over the set of clusters. Hence the sub-channels make use of the preference values send by the clusters to make decisions.

B. One-to-One Matching Algorithm for MC-NOMA

After the initial power allocation, each user calculates the rate on each sub-channel using (6). In order to build the preference profiles, the clusters then evaluate $Q^m[c]$ on all sub-channels. The preference profile of each cluster is independent of the other. The clusters then rank the sub-channels in a increasing order to have priority value over each sub-channel. The next step is to match the clusters and the sub-channels based on the *deferred acceptance* algorithm [35].

In our algorithm, the clusters propose the sub-channels based upon their preference profiles. Initially, each cluster proposes its top-ranked sub-channel. Then, each sub-channel that received proposals from more than one cluster, accepts the top-ranked proposal. The acceptance process is based on a priority value and in case of ties, the sub-channel accepts the proposal of one cluster randomly and rejects the proposals of rest of the clusters. The clusters whose proposals have been rejected by the sub-channels, proposes to their remaining top-ranked sub-channels. The convergence occurs when every cluster is allocated a distinct sub-channel. The proposed stable matching approach is summarized as Algorithm 1.

In the proposed algorithm, the matching of clusters to sub-channels obeys the preferences and therefore it is a *stable matching*. Formally, a stable match is defined as follows

Definition 3: Consider two sub-channels c and c' which are matched to clusters m and m', respectively. This matching is stable if c prefers m to m' and m prefers c to c' [36].

Hence, the proposed sub-channel assignment approach always converges to a stable match between the clusters and sub-channels.

Algorithm 2 The Proposed Algorithm for Power Allocation

For given cluster with sub-channel allocation, initialize K_m, P_c, R_{min}, δ, β, ϵ, $p_k^m[c]$, $\zeta_k^m[c]$, π_k^m, μ_k^m, η_k^m, ω_k^m and $z = 0$.
while π_k^m, μ_k^m, η_k^m and ω_k^m have not converged
Calculate $p_k^m[c]^*$ using (19).
Update π_k^m, μ_k^m, η_k^m and ω_k^m using (20), (21), (22) and (23).
Select the step size as $\psi(z) = \frac{z}{2z+1}$.
Iterate $z = z + 1$.
Repeat these steps until convergence.
End **while**

V. Proposed Solution for power allocation

After the sub-channel allocation, the original problem **(P)** is reformulated for power allocation of each cluster as follows

$$\begin{aligned}
&(\mathbf{P2}): \underset{p_k^m[c]}{\text{maximize}} \sum_{k=1}^{K_m}\sum_{c=1}^{C} R_k^m[c] \\
&\text{subject to:} \\
&\widehat{C}_1: R_k^m[c] \geq R_{min}, \forall k \\
&\widehat{C}_2: \sum_{k=1}^{K_m} p_k^m[c] \leq P_c = P_{BS}/C, \\
&\widehat{C}_3: p_k^m[c] \geq 0, \forall k \\
&\widehat{C}_4: \sum_{i=1}^{k-1} p_i^m[c] + \frac{\beta}{\mid h_{k-1}^m[c] \mid^2} \leq p_k^m[c], \forall k \\
&\widehat{C}_5: \left(R_1^m[c] - R_k^m[c] \right) \leq \delta, \forall k
\end{aligned} \tag{15}$$

The problem **(P2)** is still a non-convex problem. Therefore, we employ the Lagrangian method to solve it. The Lagrangian function for **(P2)** is given as

$$\begin{aligned}
&\mathcal{L}(p, \boldsymbol{\pi}, \boldsymbol{\mu}, \boldsymbol{\eta}, \boldsymbol{\omega}) = \\
&\sum_{k=1}^{K_m} R_k^m[c] + \sum_{k=1}^{K_m} \pi_k^m \left(R_k^m[c] - R_{min}\right) + \sum_{k=1}^{K_m} \mu_k^m \left(P_c - p_k^m[c]\right) \\
&+ \sum_{k=1}^{K_m} \eta_k^m \left(p_k^m[c] - \sum_{i=1}^{k-1} p_i^m[c] - \frac{\beta}{\mid h_{k-1}^m[c] \mid^2} \right) \\
&+ \sum_{k=1}^{K_m} \omega_k^m \left(\delta + R_k^m[c] - R_1^m[c]\right).
\end{aligned} \tag{16}$$

where $\pi_k^m, \mu_k^m, \eta_k^m$ and ω_k^m, denote the positive Lagrangian multipliers.

The Lagrangian function in (16) is solved for optimal power by first applying the Karush-Kahn-Tuck (KKT) conditions and then solving the Lagrangian multipliers using the sub-gradient method. Now by applying the KKT conditions to (16) and taking the partial derivative w.r.t $p_k^m[c]$, we get

$$\frac{\partial \mathcal{L}(.)}{\partial p_k^m[c]} = \frac{(1 + \omega_k^m + \pi_k^m)\, \zeta_k^m[c]}{\ln 2\,(1 + p_k^m[c]\zeta_k^m[c])} - \mu_k^m + \eta_k^m - \Phi_k^m[c], \tag{17}$$

where $\Phi_k^m[c]$ and $\zeta_k^m[c]$ are defined as

$$\Phi_k^m[c] = \sum_{j=k+1}^{K_m} \left(\eta_j^m + \frac{(1 + \pi_j + \omega_j) p_j^m \zeta_j^m[c]^2}{\ln 2 (1 + p_j^m[c]\zeta_j^m[c])} \right) \tag{19}$$

$$\zeta_k^m[c] = \frac{\mid h_k^m[c] \mid^2}{\mid h_k^m[c] \mid^2 I_k^m[c] + \sigma^2}, \tag{18}$$

By setting $\frac{\partial \mathcal{L}(.)}{\partial p_k^m[c]} = 0$, the optimal power $p_k^m[c]^*$ is obtained as

$$p_k^m[c]^* = \left[\frac{(1 + \omega_k^m + \pi_k^m)}{\ln 2 (\mu_k^m - \eta_k^m + \Phi_k^m[c])} - \frac{1}{\zeta_k^m[c]} \right]^+, \tag{20}$$

where $(\Lambda)^+ = \max(0, \Lambda)$. The Lagrangian multipliers determined using the sub-gradient method are given as

$$\pi_k^m(z+1) = \left[\pi_k^m(z) - \psi(z) \left(R_k^m[c] - R_{min} \right) \right]^+, \forall k, \tag{21}$$

$$\mu_k^m(z+1) = \left[\mu_k^m(z) - \psi(z) \left(P_c - \sum_{k=1}^{K_m} p_k^m[c] \right) \right]^+, \tag{22}$$

$$\begin{aligned}
\eta_k^m(z+1) = \Bigg[\eta_k^m(z) - \psi(z) \Bigg(p_k^m[c] - \sum_{i=1}^{k-1} p_i^m[c] \\
- \frac{\beta}{\mid h_{k-1}^m[c] \mid^2} \Bigg) \Bigg]^+, \forall k \in \{2, 3, ..., K_m\},
\end{aligned} \tag{23}$$

$$\begin{aligned}
\omega_k^m(z+1) = \left[\omega_k^m(z) - \psi(z) \left(\delta + R_k^m[c] - R_1^m[c] \right) \right]^+, \\
\forall k \in \{2, 3, ..., K_m\},
\end{aligned} \tag{24}$$

where $\psi(z) = \frac{z}{2z+1}$, is the positive step size [32] and z denotes the iteration number. In each iteration of z, $\pi_k^m, \mu_k^m, \eta_k^m$ and ω_k^m are updated using $p_k^m[c]^*$ and optimal values of $\pi_k^m, \mu_k^m, \eta_k^m$ and ω_k^m are used to obtain $p_k^m[c]^*$ in the subsequent iteration. The process continues until the convergence occurs, i.e., the difference between two consecutive values of multipliers is less than ϵ. The proposed power allocation algorithm is summarized as Algorithm 2.

VI. Simulation results and discussion

In this section, simulation results and their discussion are provided to evaluate the performance of our proposed scheme. Our simulation results compare the following four approaches:
1) Approach A: This is the proposed channel assignment and power allocation approach.
2) Approach B: This represents the channel selection based on maximum sum rate followed by optimal power allocation without rate fairness constraint.
3) Approach C: This represents the channel selection based on minimum power requirement followed by optimal power allocation without rate fairness constraint.
4) Approach D: It denotes the proposed channel assignment approach followed by optimal power allocation without rate fairness constraint.

To better demonstrate the performance of our proposed approach with IRS, we consider that the direct links from BS

Table I. Simulation Parameters

Paramter	Definition	Value
C	Number of channels	5
M	Number of clusters	5
K_m	Number of users per cluster	3
P_{BS}	Maximum BS power	5 W
G_t and G_r	Antenna gains	10 dBi
σ^2	Noise Power	-94 dBm
β	Minimum power gap for successful SIC	10 dBm
δ	Rate Fairness Factor	1 - 2 bps/Hz
R_{min}	Per user QoS requirement	0.25 - 1.5 bps/Hz
N	Number of IRS reflecting elements	20 - 50

to users are strongly attenuated for all clusters, hence they take help from IRS to establish communication. The simulation parameters are enlisted in Table I.

Fig. 2 depicts the sum rate of the network versus the increasing QoS requirement. We can observe that the proposed approach outperforms the other approaches. This is because the proposed approach not only satisfies the QoS requirement but also balances the rates of users in each cluster. The difference in the sum rates of Approach B, C and D is due to the sub-channel selection criteria. The Approach B selects the channel based on maximum sum rate which leads to a higher network sum rate than Approach C and D and the Approach D has minimum sum rate because for this approach cluster prefers the channel for which the difference between the rates of the strongest and the weakest user is minimum. As the QoS requirement increases, the sum rate for each approach increases but the Approach B, C and D do not ensure the rate fairness within each cluster. This factor is highlighted in Fig. 7, where we analyze the rate of individual user within a cluster. More specifically, we fix the QoS requirement to $R_{min} = 1$ bps/Hz. It can be seen that the gap between the rates of $\mathcal{U}_1^1$ and $\mathcal{U}_2^1$ is about 2.7 bps/Hz for Approach B, C and D. Similarly, the rate gap of $\mathcal{U}_1^1$ and $\mathcal{U}_3^1$ is 3.5 bps/Hz, 3.4 bps/Hz and 3 bps/Hz for Approach B, C and D, respectively. This demonstrate that with Approach B, C and D, the users $\mathcal{U}_2^1$ and $\mathcal{U}_3^1$ are deprived of good services while only the strongest user, i.e., $\mathcal{U}_1^1$ experiences good service. Whereas, for Approach A, the gap between the rates of $\mathcal{U}_1^1$ and $\mathcal{U}_2^1$ is 0.9 bps/Hz and the gap between the rates of $\mathcal{U}_1^1$ and $\mathcal{U}_3^1$ is 1 bps/Hz. This shows that with our proposed approach, all users experience similar services. For our proposed approach, the rate of $\mathcal{U}_1^1$ is 3.9 bps/Hz, followed by $\mathcal{U}_2^1$ with 3.1 bps/Hz and the rate of $\mathcal{U}_3^1$ is 2.9 bps/Hz. Although the Approach B, C and D satisfy the QoS requirement of each user but these approaches lead to unfair resource allocation for intermediate and weak users, i.e., $\mathcal{U}_2^1$ and $\mathcal{U}_3^1$, respectively. While our proposed approach ensures a fair resource allocation and also provides maximum sum rate.

To further evaluate the performance of our proposed approach, it is important to observe the effect of varying the

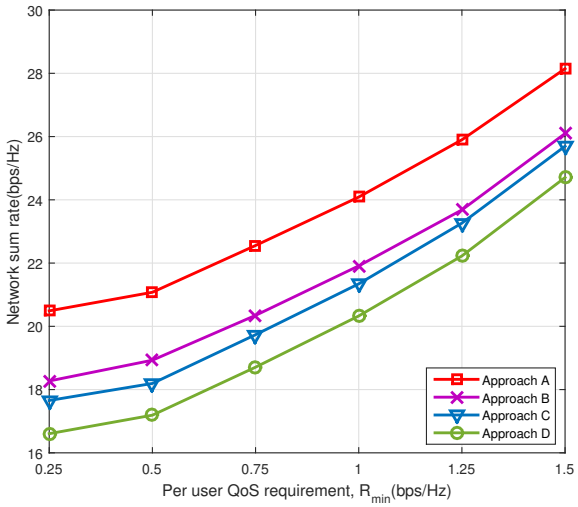

Fig. 2. The network sum rate versus per user QoS requirement for $N = 50$ and $\delta = 1$ bps/Hz.

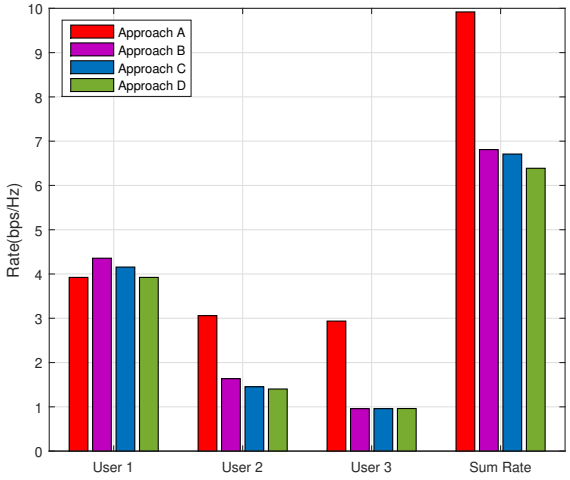

Fig. 3. Achievable rate comparison of first cluster with $R_{min} = 1$ bps/Hz, $N = 50$ and $\delta = 1$ bps/Hz for different approaches.

fairness factor, i.e., δ, on the network sum rate. Fig. 4 depicts the sum rate for different QoS requirements versus the rate fairness factor for a fixed number of IRS reflecting elements. It demonstrates that the sum rate increases with an increase in QoS requirement and decrease in fairness factor. By keeping the fairness factor constant, for example, when $\delta = 1.5$ bps/Hz, the sum rate achieved at $R_{min} = 0.5$ bps/Hz is 20.5 bps/Hz while for $R_{min} = 0.75$ bps/Hz the sum rate is is 22.25 bps/Hz and for $R_{min} = 1$ bps/Hz it is 23.25 bps/Hz. Now, by keeping the QoS requirement fixed, the network sum rate increases by decreasing the fairness factor. This is because the decrease in fairness factor ensures better rate fairness as it reduces the gap between the rates of users within each cluster. The intermediate and weak users approach the rate of strongest

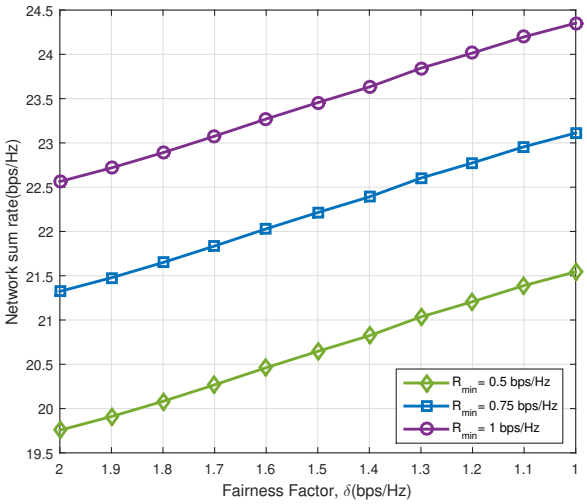

Fig. 4. The network sum rate with different values of R_{min} versus the fairness factor for $N = 50$.

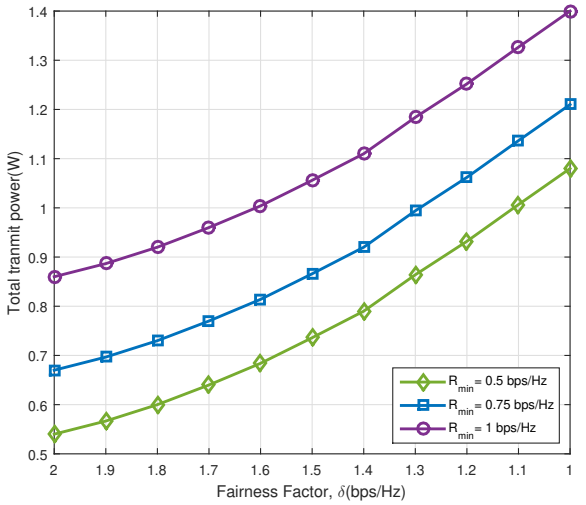

Fig. 5. The total transmit power with different values of R_{min} versus the fairness factor for $N = 50$.

user with a decrease in the fairness factor. This result illustrates positive behavior of our proposed approach.

Fig. 5 illustrates the impact of varying QoS requirement and fairness index on total transmit power. It can be seen that the total transmit power increases with an increase in QoS requirement and decrease in fairness factor. As mentioned before, smaller the value of fairness factor greater the rate fairness. Hence, in order to reduce the gap between the rates of users, the rate of weak and intermediate users approach the rate of strongest user. Therefore, more power is needed to satisfy the fairness factor.

Furthermore, Fig. 6 demonstrates the impact of fairness index on the rate of individual user within the cluster for a fixed QoS requirement. It can be seen that the rate of strongest user, i.e., $\mathcal{U}_1^1$, is not affected by varying δ. As δ varies from 2 bps/Hz to 1 bps/Hz, the rates of $\mathcal{U}_2^1$ and $\mathcal{U}_3^1$ approach the rate of $\mathcal{U}_1^1$. For $\delta = 2$ bps/Hz, the rates of $\mathcal{U}_1^1$, $\mathcal{U}_2^1$ and $\mathcal{U}_3^1$ are 3.8 bps/Hz, 2 bps/Hz and 1.8 bps/Hz, respectively. This shows that for larger values of δ, $\mathcal{U}_2^1$ and $\mathcal{U}_3^1$ are deprived of service that $\mathcal{U}_1^1$ experiences. While for $\delta = 1$ bps/Hz, the rates of $\mathcal{U}_2^1$ and $\mathcal{U}_3^1$ are 3 bps/Hz and 2.8 bps/Hz, respectively, hence now $\mathcal{U}_2^1$ and $\mathcal{U}_3^1$ also experience good services as $\mathcal{U}_1^1$. This shows that our proposed approach ensures user fairness so that all users experience similar services. Moreover, it can be observed that with the decrease in the value δ, the sum rate of the cluster also increases. Hence, the network operator can adjust the value of δ according to the requirement.

To show the performance of our proposed approach for increasing IRS reflecting elements, Fig. 7 investigates the network sum rate and total transmit power for increasing IRS reflecting elements, where QoS requirement and rate fairness factor are kept constant. It is observed that the network sum rate increases with increasing number of IRS elements. This indicates that a large number of IRS elements leads to more power gain as they can reflect more signal power received from the BS. Similarly, the total transmit power decreases

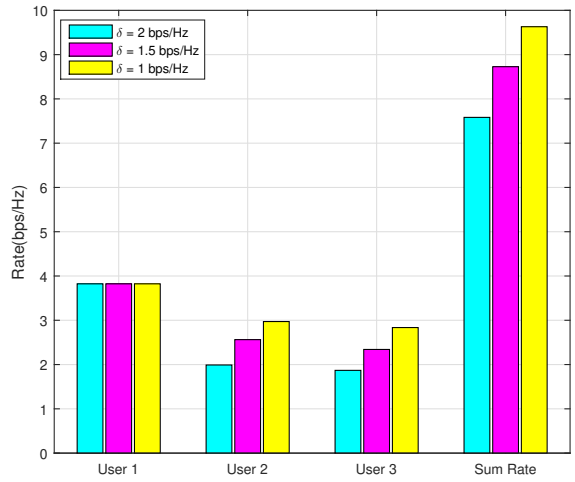

Fig. 6. Achievable rate comparison of first cluster with different values of δ for $R_{min} = 1$ bps/Hz and $N = 50$.

with increasing number of IRS reflecting elements. The power gain added by large number of IRS elements leads to low transmit power to satisfy the QoS and rate fairness constraints. It is noted that the decrease in total transmit power with an increasing number of IRS elements is not constant. For instance, there is 1.2 W decrease when IRS reflecting elements increase from 20 to 35 and only 0.1 W decrease when IRS elements are further increased. This is due to the rate fairness constraint that tries to ensure minimum gap between the rates of users in each cluster. As the number of IRS elements increases, the rate of the strong users increases more. Hence, more power is needed by other users in the cluster to satisfy the rate fairness constraint. Therefore, we can get higher network sum rate at low transmit power by increasing the number of IRS reflecting elements.

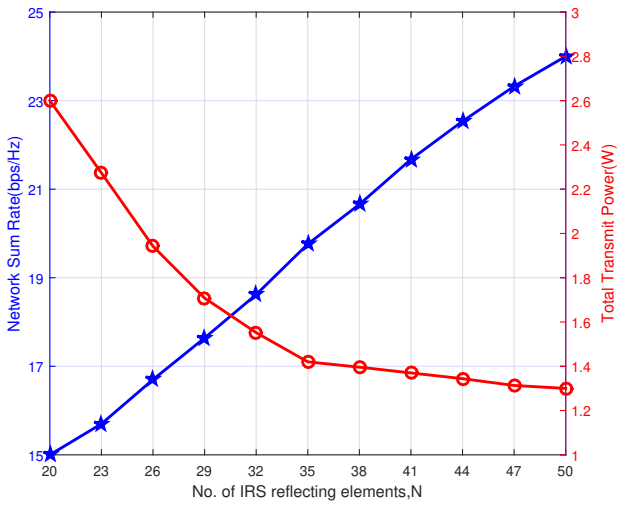

Fig. 7. The network sum rate and total transmit power versus the increasing number IRS reflecting elements for $R_{min} = 1$ bps/Hz and $\delta = 1$ bps/Hz.

VII. Conclusion

A resource allocation problem of IRS-aided downlink MC-NOMA system has been studied in this paper. A sum rate maximization problem under QoS and rate fairness constraints was formulated by jointly optimizing the sub-channel assignment and power allocation. Specifically, the original problem was split into two sub-problems and solved in sequence where: 1) a sub-channel assignment algorithm based on matching theory has been proposed, which always achieves a stable match between the clusters and the sub-channels; 2) a Lagrangian-based power allocation algorithm is proposed, which first utilizes the KKT conditions to determine the Lagrangian multipliers and then achieves convergence using sub-gradient method. Our simulation results demonstrate that the proposed algorithm shows superior performance in terms of network sum rate and user fairness. Moreover, our results show that more number of IRS elements add power gain, which enhances the system performance. In future, we would like to investigate the joint optimization of number of IRS reflecting elements and IRS phase shift matrix along with the sub-channel assignment and power allocation.

References

[1] S. Lien, S. Shieh, Y. Huang, B. Su, Y. Hsu, and H. Wei, "5G New Radio: Waveform, Frame Structure, Multiple Access, and Initial Access", *IEEE Communications Magazine*, vol. 55, no. 6, pp. 64–71, 2017.

[2] S. Parkvall, E. Dahlman, A. Furuskar, and M. Frenne, "NR: The New 5G Radio Access Technology", *IEEE Communications Standards Magazine*, vol. 1, no. 4, pp. 24–30, 2017.

[3] W. Tang, M. Z. Chen, X. Chen, J. Y. Dai, Y. Han, M. Di Renzo, Y. Zeng, S. Jin, Q. Cheng, and T. J. Cui, "Wireless Communications With Reconfigurable Intelligent Surface: Path Loss Modeling and Experimental Measurement", *IEEE Transactions on Wireless Communications*, vol. 20, no. 1, pp. 421–439, 2021. DOI: 10.1109/TWC.2020.3024887.

[4] Q. Wu and R. Zhang, "Intelligent Reflecting Surface Enhanced Wireless Network via Joint Active and Passive Beamforming", *IEEE Transactions on Wireless Communications*, vol. 18, no. 11, pp. 5394–5409, 2019.

[5] ——, "Towards Smart and Reconfigurable Environment: Intelligent Reflecting Surface Aided Wireless Network", *IEEE Communications Magazine*, vol. 58, no. 1, pp. 106–112, 2020.

[6] S. Basharat, M. Khan, M. Iqbal, S. Zaidi, U. Hashmi, and I. Robertson, "Exploring Reconfigurable Intelligent Surfaces for 6G: State-of-the-Art and the Road Ahead", *IET Communications*, 2022.

[7] M. Jung, W. Saad, Y. Jang, G. Kong, and S. Choi, "Performance Analysis of Large Intelligent Surfaces (LISs): Asymptotic Data Rate and Channel Hardening Effects", *IEEE Transactions on Wireless Communications*, vol. 19, no. 3, pp. 2052–2065, 2020. DOI: 10.1109/TWC.2019.2961990.

[8] Z. Ding, Y. Liu, J. Choi, Q. Sun, M. Elkashlan, C.-L. I, and H. V. Poor, "Application of Non-Orthogonal Multiple Access in LTE and 5G Networks", *IEEE Communications Magazine*, vol. 55, Nov. 2015.

[9] S. Zeb, Q. Abbas, S. A. Hassan, A. Mahmood, and M. Gidlund, "Enhancing Backscatter Communication in IoT Networks with Power-Domain NOMA", in *Wireless-Powered Backscatter Communications for Internet of Things*, Springer, 2020, pp. 81–101.

[10] K. Higuchi and A. Benjebbour, "Non-orthogonal Multiple Access (NOMA) with Successive Interference Cancellation for Future Radio Access", *IEICE Trans. Commun.*, vol. 98, no. 3, pp. 403–414, 2015.

[11] Z. Ding, Z. Yang, P. Fan, and H. V. Poor, "On the Performance of Non-Orthogonal Multiple Access in 5G Systems with Randomly Deployed Users", *IEEE Signal Processing Letters*, vol. 21, no. 12, pp. 1501–1505, 2014.

[12] S. Zeb, Q. Abbas, S. A. Hassan, A. Mahmood, R. Mumtaz, S. H. Zaidi, S. A. R. Zaidi, and M. Gidlund, "NOMA Enhanced Backscatter Communication for Green IoT Networks", in *2019 16th International Symposium on Wireless Communication Systems (ISWCS)*, IEEE, 2019, pp. 640–644.

[13] J. A. Oviedo and H. R. Sadjadpour, "A Fair Power Allocation Approach to NOMA in Multiuser SISO Systems", *IEEE Transactions on Vehicular Technology*, vol. 66, no. 9, pp. 7974–7985, 2017.

[14] Y. Sun, D. W. K. Ng, Z. Ding, and R. Schober, "Optimal Joint Power and Subcarrier Allocation for Full-Duplex Multicarrier Non-Orthogonal Multiple Access Systems", *IEEE Transactions on Communications*, vol. 65, no. 3, pp. 1077–1091, 2017.

[15] F. Fang, H. Zhang, J. Cheng, and V. C. M. Leung, "Energy-Efficient Resource Allocation for Downlink Non-Orthogonal Multiple Access Network", *IEEE Transactions on Communications*, vol. 64, no. 9, pp. 3722–3732, 2016.

[16] Z. Zhang, Y. Cui, F. Yang, and L. Ding, "Analysis and optimization of outage probability in multi-intelligent reflecting surface-assisted systems", *arXiv preprint arXiv:1909.02193*, 2019.

[17] Ö. Özdogan, E. Björnson, and E. G. Larsson, "Intelligent Reflecting Surfaces: Physics, Propagation, and Pathloss Modeling", *IEEE Wireless Communications Letters*, vol. 9, no. 5, pp. 581–585, 2019.

[18] E. Björnson, Ö. Özdogan, and E. G. Larsson, "Intelligent Reflecting Surface Versus Decode-and-Forward: How Large Surfaces Are Needed to Beat Relaying?", *IEEE Wireless Communications Letters*, vol. 9, no. 2, pp. 244–248, 2019.

[19] D. Mishra and H. Johansson, "Channel Estimation and Low-complexity Beamforming Design for Passive Intelligent Surface Assisted MISO Wireless Energy Transfer", in *Proc. IEEE International Conference on Acoustics, Speech and Signal Processing (ICASSP)*, 2019, pp. 4659–4663.

[20] Q. Nadeem, H. Alwazani, A. Kammoun, A. Chaaban, M. Debbah, and M. Alouini, "Intelligent Reflecting Surface-Assisted Multi-User MISO Communication: Channel Estimation and Beamforming Design", *IEEE Open Journal of the Communications Society*, vol. 1, pp. 661–680, 2020.

[21] Q. Zhang, W. Saad, and M. Bennis, "Reflections in the Sky: Millimeter Wave Communication with UAV-Carried Intelligent Reflectors", in *IEEE Global Communications Conference (GLOBECOM)*, 2019, pp. 1–6.

[22] X. Jia, J. Zhao, X. Zhou, and D. Niyato, "Intelligent Reflecting Surface-Aided Backscatter Communications", *arXiv preprint arXiv:2004.09059*, 2020.

[23] C. Pan, H. Ren, K. Wang, M. Elkashlan, A. Nallanathan, J. Wang, and L. Hanzo, "Intelligent Reflecting Surface Aided MIMO Broadcasting for Simultaneous Wireless Information and Power Transfer", *IEEE Journal on Selected Areas in Communications*, 2020.

[24] B. Lyu, D. T. Hoang, S. Gong, D. Niyato, and D. I. Kim, "IRS-Based Wireless Jamming Attacks: When Jammers Can Attack Without Power", *IEEE Wireless Communications Letters*, vol. 9, no. 10, pp. 1663–1667, 2020. DOI: 10.1109/LWC.2020.3000892.

[25] Z. Ding, R. Schober, and H. V. Poor, "On the Impact of Phase Shifting Designs on IRS-NOMA", *IEEE Wireless Communications Letters*, vol. 9, no. 10, pp. 1596–1600, 2020. DOI: 10.1109/LWC.2020.2991116.

[26] B. Zheng, Q. Wu, and R. Zhang, "Intelligent Reflecting Surface-Assisted Multiple Access With User Pairing: NOMA or OMA?", *IEEE Communications Letters*, vol. 24, no. 4, pp. 753–757, 2020.

[27] J. Zhu, Y. Huang, J. Wang, K. Navaie, and Z. Ding, "Power Efficient IRS-Assisted NOMA", *IEEE Transactions on Communications*, vol. 69, no. 2, pp. 900–913, 2021. DOI: 10.1109/TCOMM.2020.3029617.

[28] Z. Ding and H. V. Poor, "A Simple Design of IRS-NOMA Transmission", *IEEE Communications Letters*, vol. vol.24, no. no.5, pp. 1–1, 2020.

[29] X. Mu, Y. Liu, L. Guo, J. Lin, and N. Al-Dhahir, "Exploiting Intelligent Reflecting Surfaces in Multi-Antenna Aided NOMA Systems", *arXiv preprint arXiv:1910.13636*, 2019.

[30] T. Hou, Y. Liu, Z. Song, X. Sun, Y. Chen, and L. Hanzo, "Reconfigurable Intelligent Surface Aided NOMA Networks", *IEEE Journal on Selected Areas in Communications*, 2020.

[31] X. Yue and Y. Liu, "Performance Analysis of Intelligent Reflecting Surface Assisted NOMA Networks", *IEEE Transactions on Wireless Communications*, vol. 21, no. 4, pp. 2623–2636, 2022. DOI: 10.1109/TWC.2021.3114221.

[32] W. U. Khan, F. Jameel, M. Jamshed, H. Pervaiz, S. Khan, and J. Liu, "Efficient Power Allocation for NOMA-enabled IoT Networks in 6G Era", *Physical Communication*, p. 101 043, Feb. 2020.

[33] L. Wolsey and G. Nemhauser, *Integer and Combinatorial Optimization*. John Wiley & Sons, USA, 2014.

[34] A. B. MacKenzie and L. A. DaSilva, *Game Theory for Wireless Engineers*. Morgan & Claypool Publishers, 2006.

[35] N. Nisan, T. Roughgarden, E. Tardos, and V. Vazirani, *Algorithmic Game Theory*. Cambridge University Press, 2007, p. 256.

[36] D. Gale and L. Shapely, "College Admissions and the Stability of Marriage", *The American Mathematical Monthly*, vol. 69, no. 1, pp. 9–15, January 1962.